CrystEngComm

Accepted Manuscript

ROYAL SOCIETY OF CHEMISTRY

www.rsc.org/crystengcomm

ARTICLE

Structural and anti-oxidant properties of guanidinium pyrazole-3,5-dicarboxylates

Received 00th January 20xx,
Accepted 00th January 20xx

DOI: 10.1039/x0xx00000x

www.rsc.org/

S. Packiaraj[a,b], A. Pushpaveni[a], S. Govindarajan*[a] and J. M. Rawson[c]

Multicomponent crystals (either salts or co-crystals) of pyrazole-3,5-dicarboxylic acid(H_3pzdc) with the nitrogen-containing organic bases guanidine(Gun), aminoguanidine(Agun), diaminoguanidine(Dagun) and triaminoguanidine(Tagun), have been synthesized and characterized by IR spectroscopy, TG-DTA, single-crystal X-ray diffraction. Aminoguanidine and diaminoguanidine exhibit three types of salts depending upon reaction conditions, comprising: (a) 1:1 salts [AgunH/DagunH][H_2pzdc]; (b) 2:1 salts generated by double deprotonation of the acid [AgunH/DagunH]$_2$[Hpzdc] and; (c) the unusual 1:2 salts [AgunH/DagunH][H_2pzdc][H_3pzdc] which comprise cocrystals of the 1:1 salt and the free acid. Interestingly Tagun forms only the 1:2 salt [TagunH][H_2pzdc][H_3pzdc], irrespective of stoichiometry. The hydrogen-bonded assemblies associated with each structure are discussed.The co-crystals of free acid and the mono-deprotonated acid have melting points distinct from both the 1:1 and 2:1 salts consistent with phase pure materials. TG-DTA studies on these salts reveal thermal degradation occurs through desolvation and loss of free organic base. Both the parent acid and its salts display a strong fluorescent emission (λ_{em} = 373-438 nm) at room temperature and their antibacterial activity, total antioxidant capacity (TAC) as well as DPPH assays of the free acid and its salts are reported. The crucial role of the hydrazinic moiety in the antibacterial and antioxidant activities is identified.

Introduction

Guanidine (Gun, Scheme 1) is biologically important as a key functional group in amino acids.[1-7] The physical properties of guanidinium salts have therefore attracted considerable interest with regard to a variety of applications in the fields of biotechnology, medicine, etc., and guanidine is one of the strongest organic nitrogenous bases known (pk_b = 0.40). Guanidine contains three amines in a planar arrangement and remains protonated over a wide pH range. The presence of multiple amine groups permits it to form up to five hydrogen bonds when present within the arginine side chain. These structural features make it a versatile moiety for molecular recognition and catalysis.[3-7] Derivatives of guanidine, such as the higher nitrogen-rich analogues *viz*. aminoguanidine(Agun), diaminoguanidine(Dagun) and triaminoguanidine(Tagun) (Scheme 1) are used in explosives and rocket propellant formulations.[8-11] However the basic nature of guanidines means that these are not normally isolated as the free base but rather as their guanidinium salts, stabilized by a range of different anions.[12-14] The presence of both imino and amino groups afford multiple basic sites for protonation leading to a diversity of potential salts with a range of acids. Typically the imino-N is more basic and guanidinium salts with chloride, nitrate, carbonate, perchlorate, phosphate, sulphate and pyrophosphate anions have been reported.[15-26] Derivatives of mono-, di- and tri-aminoguanidinium salts with various anions such as Cl^-, NO_3^-, SO_3^{2-}, picrate, perchlorate, *N,N*-dinitro-1,2-ethanediamino salts and $H_2PO_4^-$ are also known.[15-30]

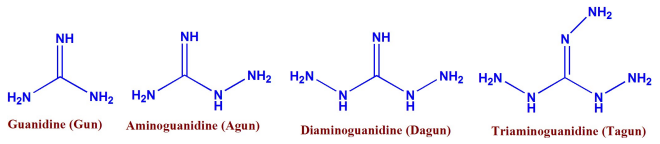

Scheme 1 The structures of guanidine bases

The crystal structures of doubly-protonated species are somewhat rarer but include aminoguanidinium(+2)-sulphate, [AgunH$_2$][SO_4], and di-nitrate, [AgunH$_2$][NO_3]$_2$.[31-33] In this latter series, not only the imino nitrogen, but also the hydrazinic nitrogen (-NH_2) become protonated and is less favoured due to loss of π-delocalisation during the second protonation. A number of preparative and computational studies on the synthesis and energetics of aminoguanidinium salts derived from *inorganic* acids have been reported.[9-11,33] The syntheses of guanidinium and/or aminoguanidinium salts of organic acids have been widely explored with few examples of *organic* salts,

[a] Department of Chemistry, Bharathiar University, Coimbatore-641 046, India. * Corresponding author; E-mail: srajguru1987@gmail.com, drsgovind@yahoo.co.in* Tel: +91 422 2428315; Fax: +91 - 422 2425706
[b] Science and Humanities (Chemistry), Sri Krishna College of Engineering & Technology, Coimbatore-641 008, India.
[c] Department of Chemistry and Biochemistry, The University of Windsor, Ontario N9B3P4, Canada.

† Footnotes relating to the title and/or authors should appear here.
Electronic Supplementary Information (ESI) available: [details of any supplementary information available should be included here]. See DOI: 10.1039/x0xx00000x

viz. formate,[34] hemi-oxalate,[35] hydrogen-L-tartrates,[36,37] squarates,[38,39] fumarates,[40-43] succinates,[44] oxalates,[45-48] benzoate,[49] maleates,[50,51] pyromelliate,[52] oxamate,[48] malonate,[48] sulfoacetate[48] and glutamate.[53] From our literature survey, we identified a small number of crystal structures with 6-membered hetero-aromaticdicarboxylic acids; the guanidinium/aminoguanidinium salts of chelidamate dipicolinates and quinolinate[54-56] reveal that the guanidinium/aminoguanidinium ions in these salts exist solely in the mono-protonated form. Notably there are no studies on 5-membered, nitrogen-rich dicarboxylic acids. In this paper we have chosen to examine salts of pyrazole-3,5-dicarboxylic acid(H_3pzdc) since this ligand possesses three different protonated hydrogen's (H_a, H_b and H_c in Scheme 2) offering differing acidities and multiple hydrogen-bonding sites in different chemical environments which makes it an interesting architectural building block from which to study supramolecular networks *via* salt/co-crystal formation. Herein we report the synthesis, structural characterization, thermal stability, luminescent properties and anti-oxidant behaviour of salts of H_3pzdc.

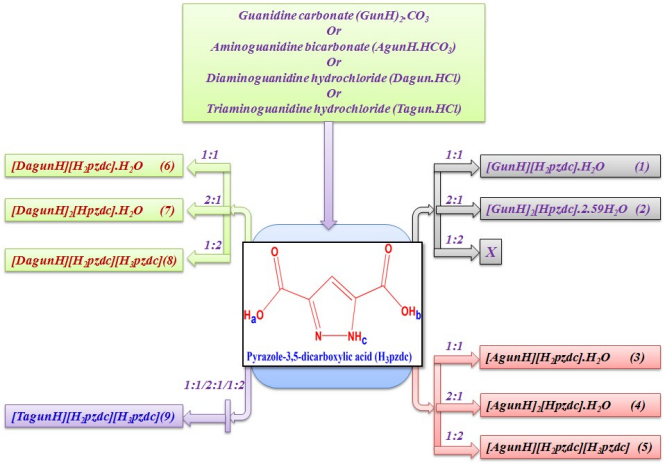

Scheme 2 The structure of pyrazole-3,5-dicarboxylic acid(H_3pzdc) and schematic representation of the different guanidinium salts obtained as a function of stoichiometry

Experimental section

Materials and physical measures

All reagents were of A.R. grade and used without further purification. The hydrazine content in all the compounds was determined volumetrically using 0.025 M KIO_3 solution under Andrews' conditions.[57] Elemental analyses for C, H, N and S were performed on a Vario-ELIII elemental analyzer. The IR spectra were recorded on a JACSO – 4100 spectrophotometer as KBr pellets in the range of 4000 – 400 cm^{-1}. Melting points were determined on MR–VIS, LABINDIA visual melting range apparatus and are uncorrected. The simultaneous TG–DTA studies were undertaken on a Perkin – Elmer SII thermal analyzer and the curves were obtained in air using platinum cup sample holders containing 5 – 10 mg of the sample a heating rate of $10^{o}C.min^{-1}$. Single crystal X-ray data for compound **1, 2** and **9** were collected on a Bruker APEX-II CCD diffractometer using Mo-K_α radiation at room temperature. Data were collected using APEX-II software,[58] integrated using SAINT[59] and corrected for absorption using SADABS.[60] Using Olex2, the structure was solved with the superflip structure solution program, using the charge flipping solution method. The structures were solved using Olex2[61] and full least-squares refinement undertaken against F^2 refined using SHELXL-2014/7 program.[62] The structure of compound **2** proved particularly problematic and subject to disorder (evidenced by high residual R values in relation to R_{int} and systematic $F_o > F_c$ in the most disagreeable reflections). Whilst the disorder was not resolved, the data quality was sufficient to identify the connectivity and gross packing features. Data for **4** was collected at -100°C on a Bruker APEX CCD diffractometer using Mo-K_α radiation. Data were collected using SMART software,[63] integrated using SAINT[59] and corrected for absorption using SADABS.[60] The structure was solved by direct methods and full least-squares refinement undertaken against F^2 using SHELXL-97 program.[62] H atoms were located in subsequent difference maps and their coordinates refined with N-H bond restraints and a riding model for their U_{iso}. CCDC deposit numbers: 955243, 955244, 1008628 and 918727. A summary of the crystallographic data and details of the final refinement parameters are summarized in Table 1**.** The luminescence spectra for the salts were recorded with a Perkin-Elmer LS-55 spectrophotometer, whose excitation and emission slit width were 10 and 5 nm, respectively.

Preparation of Guanidinium salts

To prepare [GunH][H_2pzdc]·H_2O and [GunH]$_2$[Hpzdc]·2.59H_2O, the stoichiometric quantities of base (0.090 g, 0.001 mol or 0.180 g, 0.002 mol) and acid (0.174 g, 0.001 mol) were mixed in 50 mL of double distilled water and heated over a water-bath to afford a clear solution. The resulting solutions (observed pH = 2.80 for 1:1, pH = 4.35 for 2:1) were allowed to crystallize by standing at room temperature. The mono-guanidinium salt [GunH][H_2pzdc]·H_2O (**1**) was separated as off-white needle shaped crystals after five days, whereas rectangular-shaped transparent crystals of the bis-guanidinium salt [GunH]$_2$[Hpzdc]·2.59H_2O (**2**) crystallized only after two weeks. These salts were separated by filtration and washed with absolute alcohol and dried in vacuum.

[GunH][H_2pzdc]·H_2O (1). Yield: 88%. m.p. 175-176°C. $^{a}\Lambda_m$: 123 $\Omega^{-1}\cdot cm^2\cdot mol^{-1}$. Anal.calcd for $C_6H_{11}N_5O_5$ (M_r = 233.20): C, 30.90%; H, 4.76%; N, 30.04%. Found: C, 30.85%; H, 4.80%; N, 30.00%. FT-IR (KBr, cm^{-1}): 3435(br,s), 1642(s), 1533(s), 1415(s), 1240(m), 1141(s), 1052(w), 945(m), 846(m), 760(m), 725(m), 673(m), 611(m), 564(m), 532(m), 431(m).

[GunH]$_2$[Hpzdc]·2.59H_2O (2). Yield: 82%. m.p. 125-127°C. $^{a}\Lambda_m$: 233 $\Omega^{-1}\cdot cm^2\cdot mol^{-1}$. Anal.calcd for $C_7H_{16}N_8O_{6.5}$ (M_r = 320.83): C, 26.17%; H, 5.91%; N, 34.89%. Found: C, 26.50%; H, 5.50%; N, 35.30%. FT-IR (KBr, cm^{-1}): 3430(br,s), 1643(s), 1528(s), 1411(s), 1247(m), 1140(s), 1056(w), 941(m), 843(m), 761(m), 723(m), 670(m), 614(m), 562(m), 531(m), 433(m).

Preparation of Aminoguanidinium salts

The aminoguanidinium salts of pyrazole-3,5-dicarboxylic acid, H_3pzdc, were prepared by mixing aminoguanidine bicarbonate (0.136 g, 0.001 mol or 0.272 g, 0.002 mol) and H_3pzdc (0.174 g, 0.001 mol or 0.348 g, 0.002 mol) in 1:1, 2:1 and 1:2 mole ratios in 50 mL of double distilled water. The resulting solution was heated over a steam bath for an hour, to afford a clear solution (pH = 2.75 for 1:1, pH = 2.20 for 1:2, pH = 4.55 for 2:1), which was left to crystallize at room temperature. For the 2:1 reaction yellow square-shaped crystals of $[AgunH]_2[Hpzdc]\cdot H_2O$ (**4**) were isolated after a week. When the reaction was repeated using 1:1 and 1:2 mole ratio of base:acid, the salt $[AgunH][H_2pzdc]\cdot H_2O$ (**3**) and complex salt $[AgunH][H_2pzdc][H_3pzdc]\cdot H_2O$ (**5**) were formed respectively. Preparation of these salts can be carried out by adjusting the molar ratios of reactants directly or by inter-conversion among the obtained compounds.

$[AgunH][H_2pzdc]\cdot H_2O$ (3). Yield: 85%. m.p. 61-63°C. $^a\Lambda_m$: 124 $\Omega^{-1}\cdot cm^2\cdot mol^{-1}$. Anal.calcd for $C_6H_{12}N_6O_5$ (M_r = 248.52): C, 28.97%; H, 4.84%; N, 33.80%; Found: C, 28.95%; H, 4.80%; N, 33.75%. By titration hydrazinic part of AgunH, calc. 12.88%, found 12.90%. FT-IR (KBr, cm^{-1}): 3442(br, s), 1628(s), 1544(s), 1410(s), 1233(m), 1131(s), 1047(w), 944(m), 838(m), 749(m), 722(m), 670(m), 613(m), 567(m), 523(m), 421(m).

$[AgunH]_2[Hpzdc]\cdot H_2O$ (4). Yield: 72%. m.p. 81-82°C. $^a\Lambda_m$: 238 $\Omega^{-1}\cdot cm^2\cdot mol^{-1}$. Anal.calcd for $C_7H_{18}N_{10}O_5$ (M_r = 322.31): C, 26.08%; H, 5.64%; N, 43.47%; Found: C, 26.05%; H, 5.60%; N, 43.50%. By titration hydrazinic part of AgunH, calc. 19.85%, found 19.80%. FT-IR (KBr, cm^{-1}): 3445(br,s), 1630(s), 1547(s), 1413(s), 1236(m), 1135(s), 1042(w), 949(m), 831(m), 745(m), 721(m), 674(m), 613(m), 564(m), 520(m), 423(m).

$[AgunH][H_2pzdc][H_3pzdc]\cdot H_2O$ (5). Yield: 79%. m.p. 221-222°C. $^a\Lambda_m$: 118 $\Omega^{-1}\cdot cm^2\cdot mol^{-1}$. Anal.calcd for $C_{11}H_{13}N_8O_8$ (M_r = 385.32): C, 34.29%; H, 3.41%; N, 29.09%; Found: C, 34.30%; H, 3.40%; N, 29.10%. By titration hydrazinic part of AgunH, calc. 8.35%, found 8.30%. FT-IR (KBr, cm^{-1}): 3448(br,s), 1635(s), 1544(s), 1416(s), 1233(m), 1137(s), 1044(w), 944(m), 836(m), 744(m), 726(m), 673(m), 611(m), 563(m), 524(m), 421(m).

Preparation of Diaminoguanidinium salts

Diaminoguanidine hydrochloride (0.125 g, 0.001 mol or 0.250 g, 0.002 mol) and pyrazole-3,5-dicarboxylic acid (0.174 g, 0.001 mol or 0.348 g, 0.002 mol), were mixed in 1:1, 1:2 or 2:1 mole ratios in double distilled water (50 mL) and heated on a water-bath to obtain a clear solution with pH = 2 – 5. Then, the volume of the clear solution was reduced to half and left to crystallize at 25 °C. Crystallization commenced after two days and continued for a week. The polycrystalline substance obtained was separated by filtration, washed and dried as before affording $[DagunH][H_2pzdc]\cdot H_2O$ (**6**), $[DagunH]_2[Hpzdc]\cdot H_2O$ (**7**) and $[DagunH][H_2pzdc][H_3pzdc]$ (**8**) depending on reaction stoichiometry (1:1, 2:1 and 1:2, respectively).

$[DagunH][H_2pzdc]\cdot H_2O$ (6). Yield: 78%. m.p. 115-116°C. $^a\Lambda_m$: 123 $\Omega^{-1}\cdot cm^2\cdot mol^{-1}$. Anal.calcd for $C_6H_{13}N_7O_5$ (M_r = 263.18): C, 27.36%; H, 4.99%; N, 37.27%; Found: C, 27.30%; H, 4.95%; N, 37.25%. By titration hydrazinic part of DagunH, calc 24.42%, found 24.35%. FT-IR (KBr, cm^{-1}): 3444(br,s), 1632(s), 1547(s), 1414(s), 1231(m), 1134(s), 1043(w), 946(m), 833(m), 746(m), 724(m), 673(m), 615(m), 563(m), 525(m), 423(m).

$[DagunH]_2[Hpzdc]\cdot H_2O$ (7). Yield: 71%. m.p. 178-180°C. $^a\Lambda_m$: 236 $\Omega^{-1}\cdot cm^2\cdot mol^{-1}$. Anal.calcd for $C_7H_{20}N_{12}O_5$ (M_r = 352.25): C, 23.84%; H, 5.73%; N, 47.69%; Found: C, 23.85%; H, 5.70%; N, 47.70%. By titration hydrazinic part of DagunH, calc. 32.32%, found 32.40%. FT-IR (KBr, cm^{-1}): 3446(br,s), 1631(s), 1538(s), 1418(s), 1233(m), 1137(s), 1040(w), 941(m), 835(m), 742(m), 726(m), 671(m), 618(m), 560(m), 524(m), 421(m).

$[DagunH][(H_2pzdc][H_3pzdc]$ (8). Yield: 81%. m.p. 175-176°C. $^a\Lambda_m$: 116 $\Omega^{-1}\cdot cm^2\cdot mol^{-1}$. Anal.calcd for $C_{11}H_{15}N_9O_8$ (M_r = 401.15): C, 32.90%; H, 3.76%; N, 31.40%; Found: C, 32.90%; H, 3.75%; N, 31.40%; By titration hydrazinic part of DagunH, calc. 15.37%, found 15.25%. FT-IR (KBr, cm^{-1}): 3443(br, s), 1635(s), 1534(s), 1413(s), 1230(m), 1135(s), 1047(w), 944(m), 832(m), 744(m), 728(m), 675(m), 613(m), 565(m), 522(m), 424(m).

Preparation of Triaminoguanidinium salt, $[TagunH][H_2pzdc][H_3pzdc]$ (9)

This followed the same procedure as the preparation of $DagunH^+$ salts described above, using tri-aminoguanidine hydrochloride. Irrespective of the mole ratio (1:1, 1:2, 2:1), square-shaped crystals of $[TagunH][H_2pzdc][(H_3pzdc]$ (**9**) were isolated after 2 days and air dried.

$[TagunH][(H_2pzdc][H_3pzdc]$ (9). Yield: 78%. m.p. 222-223°C. $^a\Lambda_m$: 114 $\Omega^{-1}\cdot cm^2\cdot mol^{-1}$. Anal.calcd for $C_{11}H_{16}N_{10}O_8$ (M_r = 413.31): C, 31.96%; H, 3.99%; N, 33.90%; Found: C, 31.90%; H, 3.95%; N, 33.85%. By titration hydrazinic part of TagunH, calc. 23.22%, found 23.20%. FT-IR (KBr, cm^{-1}): 3445(br,s), 1631(s), 1537(s), 1415(s), 1233(m), 1131(s), 1048(w), 942(m), 831(m), 746(m), 723(m), 672(m), 615(m), 567(m), 520(m), 423(m).

Total antioxidant activity

The assay is based on the reduction of Mo^{VI} to Mo^{V} by the extraction and subsequent formation of a green phosphate/Mo(V) complex at acidic pH.[64] The samples at various concentrations ranging from 50 to 250 µg/mL were combined with 3 mL of reagent solution (0.6 M sulphuric acid, 28 mM sodium phosphate and 4 mM ammonium molybdate). The tubes containing the reaction solution were incubated at 90°C for 90 min. Then the absorbance of the solution was measured at 695 nm against a blank MeOH solution after cooling to room temperature. Ascorbic acid equivalents were calculated using a standard graph of ascorbic acid. All experiments were conducted in triplicate and values are expressed as equivalents of ascorbic acid in µg per mg of sample.

1,1-Diphenyl-2-picrylhydrazyl (DPPH) radical scavenging activity

DPPH radical scavenging activity was assessed according to the method of Nagendra *et al*.[65] The samples at various concentrations ranging from 20 to 100 µg/mL were mixed in 1 mL of freshly prepared 0.5 mM DPPH methanolic solution and 2 mL of 0.1 M acetate buffer, pH 5.5. The mixture was shaken followed by incubating at room temperature for 30 minutes in dark and measured calorimetrically at 517 nm. Lower absorbance at 517 nm represents higher DPPH scavenging activity. The % DPPH radical scavenging activity of samples was calculated from the decrease in absorbance at 517 nm as compared with standard ascorbic acid. Experiments were done in triplicate and the DPPH radical concentration was calculated using the following equation:

$$\text{DPPH scavenging effect } (\%) = \frac{A^0 - A^1}{A^0} \times 100$$

Where A^0 was the absorbance of the control and A^1 was the absorbance in the presence of the sample.

Results and Discussion

Pyrazole-3,5-dicarboxylic acid, H_3pzdc, is a tri-basic[66] acid comprising two carboxylic protons and one less acidic N-H proton. The pk_a value for the parent pyrazole-3-carboxylic acid is found to be 3.84 (*cf.* PhCOOH at 4.21)[67] and the dicarboxylic acid H_3pzdc is expected to have a first pk_a value (pk_{a1}) less than 3.84 and a second pk_a (pk_{a2}) more than 3.84. As a consequence, treatment with organic bases suggests the possibility to form both 1:1 and 2:1 salts with 3:1 salts unlikely unless in very strongly basic solution. The pk_a value of the guanidinium cation, $[C(NH_2)_3]^+$ (pk_a= 13.6)[68] appeared sufficiently high and therefore drive both mono- and double-deprotonation of H_3pzdc. Reaction of H_3pzdc, with the guanidine bases Gun, Agun and Dagun led to mono-deprotonation (1:1 mole ratio) and double deprotonation (1:2 mole ratio) of the acid affording [BaseH][H_2pzdc]·H_2O(**1**, **3** and **6**) and [BaseH]$_2$[Hpzdc]·nH_2O(**2**, **4** and **7**), respectively. These salts form as hydrates which were characterized by IR spectroscopy, combined TG-DTA studies and ionic conductivity as well as elemental analysis. In addition the structures of **1**, **2** and **4** have been confirmed by X-ray diffraction. In the presence of excess H_3pzdc (i.e. base:acid ratio = 1:2) the guanidine bases Agun (pk_a= 11.5), Dagun (pk_a~ 10) and Tagun (pk_a= 9.75)[33,69,70] all form non-solvated co-crystal complexes of formula [BaseH][H_2pzdc][H_3pzdc] (**5**, **8** & **9**) with the structure of **9** determined by X-ray diffraction. Both [BaseH][H_2pzdc]·H_2O and [BaseH]$_2$[Hpzdc]·H_2O salts are highly soluble in water whereas the acid rich salts [BaseH][H_2pzdc][H_3pzdc] are only slightly soluble at room temperature. Notably, in the case of Tagun, the stability of [TagunH][H_2pzdc][H_3pzdc] appears to entirely preclude formation of the corresponding 1:1 and 2:1 complexes observed for Gun, Agun and Dagun.

Electrolytic behavior of the free acid and its salts were obtained in aqueous medium. Pyrazole-3,5-dicarboxylic acid, being a slowly soluble substance, affords a value of 118 $\Omega^{-1}\cdot cm^2\cdot mol^{-1}$ corresponding to its existence as a 1:1 electrolyte. Its mono-and bis salts exhibit values of 122 -125 and 235-240 $\Omega^{-1}\cdot cm^2\cdot mol^{-1}$ respectively (reflecting 1:1 and 2:1 electrolyte behaviour). The acid-rich salts dissociate completely in hot water and shows molar conductance values around 115 $\Omega^{-1}\cdot cm^2\cdot mol^{-1}$ indicating its 2:2/1:1 electrolytic nature. The poor solubility of acid-rich salts in water may be the reason for these lower conductance values.

IR spectra

For comparison, the spectra of the starting materials and their salts have been analyzed by means of FT-IR spectroscopy and provides a useful probe to determine whether the carboxylate (-COO^-) groups are protonated and/or deprotonated. The important infrared absorption bands of the acid and salts along with their band assignments are provided in the electronic supplementary information as representative examples (Figs. S1-4, ESI). The broad features in the 3000-3500 cm^{-1} region correspond to the stretching vibrations of the NH and OH groups participating in N-H...O type hydrogen bonds.[71] The broad intense band observed in the region 3315 - 3470 cm^{-1} in all the mono and di-salts can be attributed to O-H stretching associated with the water of hydration. The bands in the region 3070 – 3360 cm^{-1} have been assigned to O-H stretching of the free acid group(s) in the case of other salts.[72] All salts exhibit asymmetric and symmetric stretching bands of the carboxylate group in the range 1570-1595 and 1360-1390 cm^{-1}, respectively.[73,74] The sharp band observed between 1690 and 1705 cm^{-1} for all the mono-guanidinium 1:1 salts containing the H_2pzdc^- anion, but which is markedly absent from 2:1 salts containing the $Hpzdc^{2-}$ di-anion, confirms the presence of the free acid group. The sharp band in the region 1110-1205 cm^{-1} for these salts is indicative of the N–N stretching mode of the hydrazinic part of the guanidinium bases.[75,76]

Structural description

The subtle difference between salt formation and/or co-crystal formation and also the different experimental conditions (acid:base ratio, pk_a, solvents, etc.,) are very important implement for chemical/pharmaceutical applications. The pk_a difference (base-acid) is a useful tool for predicting salt or co-crystal formation with larger Δpk_a differences (>3) leading to salt formation, and smaller Δpk_a values (<0) affording co-crystal formation.[77,78] In the Δpk_a range 0 – 3 the distinction between co-crystal and salt formation is less clear cut. The differences in pk_a values between the base and acid in all salts examined in this study were greater than 3, favouring proton transfer. Indeed guanidinium salt formation is not uncommon, with more than forty guanidiniumdicarboxylate salts crystallographically characterized.[34-56] The structures of [GunH][H_2pzdc]·H_2O (**1**), [GunH]$_2$[Hpzdc]·2.59H_2O (**2**), [AgunH]$_2$[Hpzdc]·H_2O (**4**) and [TagunH][H_2pzdc][H_3pzdc] (**9**) were determined by X-ray diffraction. Crystal data are presented in Table 1 with selected bond parameters presented in Tables S1-2 (ESI). The molecular structures of salts **1, 2, 4** and **9** are shown in Figure 1.

The 1:1 salt [GunH][H_2pzdc]·H_2O (**1**) crystallizes in the monoclinic space group *C2/c* with one guanidinium cation, one

pyrazole-3,5-dicarboxylate anion and one water molecule in the asymmetric unit. The H atoms were located in the difference electron-density maps and reveal proton transfer from one of the two carboxylic acid groups of the pyrazoledicarboxylic acid to the guanidine moiety, consistent with salt formation. This was confirmed by the C-O bond distances, $d_{C\text{-}O}$, of the carboxylate group 1.249(13)-1.266(13) Å in relation to the carboxylic acid functionality which are more asymmetric (1.215(14) and 1.298(13) Å) and similar to those reported for the ammonium, and hydrazonium or hydrazine-diium pyrazole-3,5-hydrogendicarboxylates.[76,79] Similarly the three crystallographically independent C-N bond lengths in the guanidinium cation are similar (1.316(15)-1.328(15) Å) consistent with proton transfer.

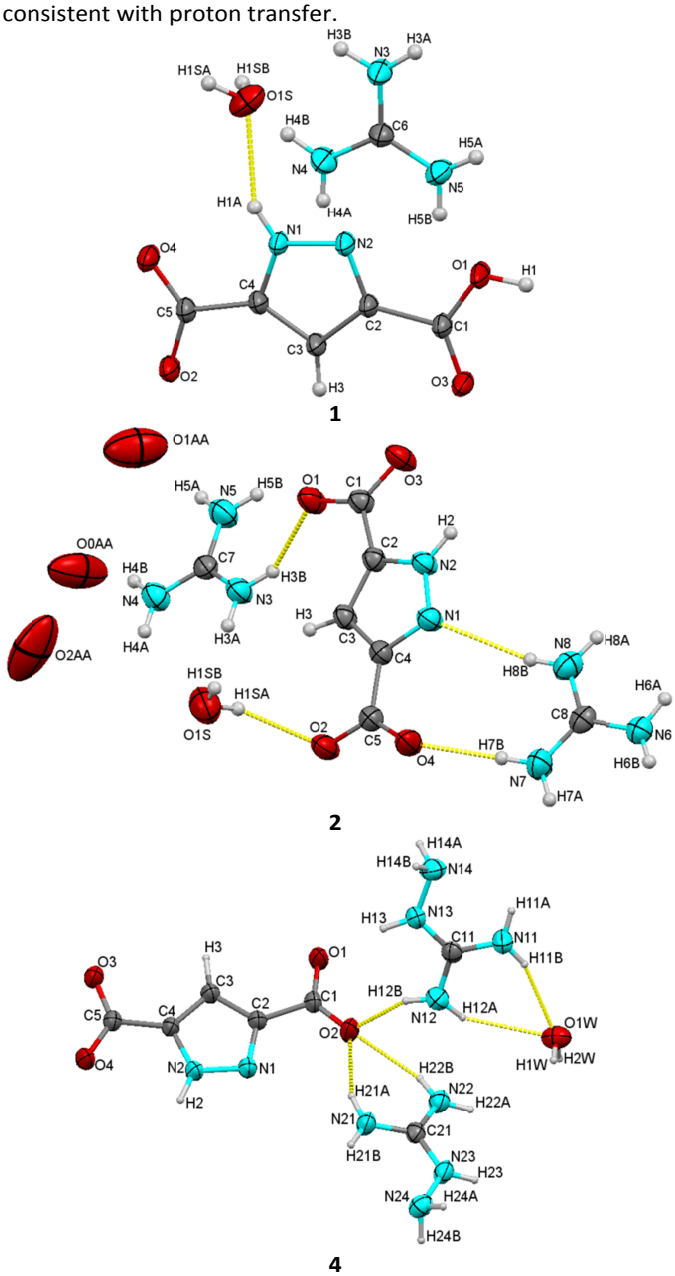

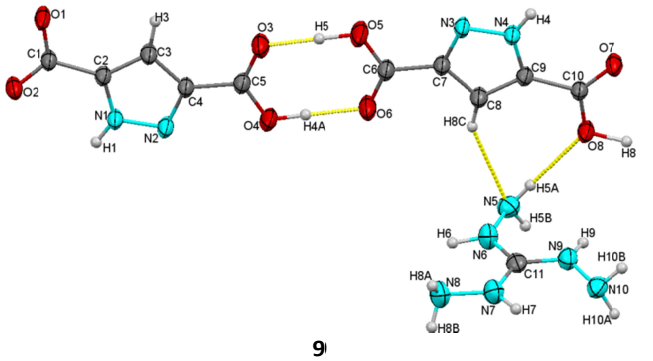

Fig. 1 Asymmetric units and atom labelling schemes for the salts **1, 2, 4** and **9** with thermal ellipsoids for non-H atoms drawn at 50% probability

The cation, anion and water molecule form a two-dimensional hydrogen bonded sheet in the crystallographic *bc* plane (Fig. 2a). The H_2pzdc^- anions are linked *via* $-CO_2H\cdots{}^-O_2C-$ hydrogen bonds to form polymeric chains parallel to the *b*-axis and a network of in-plane cation-anion hydrogen-bonded contacts link these chains along the *c*-axis (Fig. 2a). These interactions involve all three guanidinium NH_2 groups; N(3) forms a pair of N-H…N and N-H…O contacts to one anion (N-H…N at 2.12(15) and N-H…O at 2.09(15) Å); N(4) acts as a bridge between anion chains with two N-H…O hydrogen bonds (N-H…O 2.14(16) – 2.31(15) Å). The third N atom, N(5), again forms two N-H…O hydrogen bonds, one to a carboxylate O (N-H…O 2.07(14) Å) and the other to the lattice water (N-H…O 2.27(14) Å). This therefore fulfils all the hydrogen-bonding capacity of the cation. The lattice water acts as a hydrogen bond acceptor from a guanidinium N-H and the remaining N-H of the H_2pzdc^- anion (N-H…O at 2.11(14) Å). In addition it acts as a hydrogen bond donor to the carboxylic acid group (O-H…O at 2.10(16) Å) (Table 2). In terms of a graph set analysis, the hydrogen bonding within the *bc* plane can be described as alternating antiparallel C(8) chains of H_2pzdc^- anions connecting to neighboring chains by bridging guanidine and water molecules. Each guanidine forms a bidentate hydrogen bond to each of two adjacent H_2pzdc^- anions in the chain below, one through a $R^1_2(6)$ ring and another one through a $R^2_2(7)$ ring. The remaining water O-H group is oriented out of the *bc*-plane and forms an O-H…O inter-layer hydrogen bond to the carboxylate group (Fig 2b), forming a bi-layer structure generating a $R^2_3(10)$ ring.

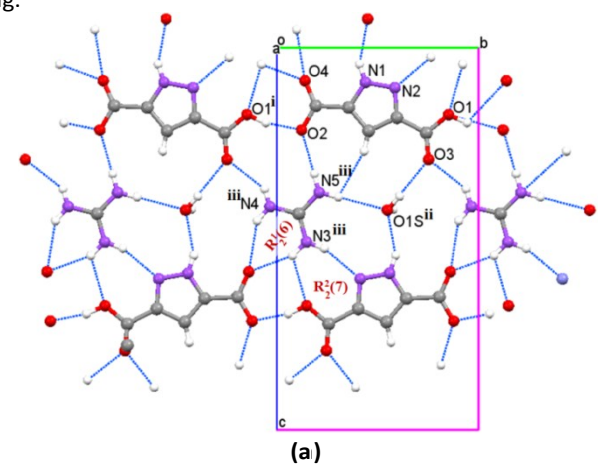

(a)

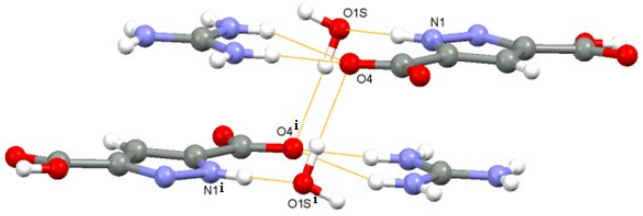

(b)

Fig. 2 (**a**) Crystal packing of **1** in the ***bc***-plane [(**i**) x, -1+y, z; (**ii**) x, 1-y, ½+z; (**iii**) ½-x, -½+y, ½-z]; (**b**) H-bonded interactions between sheets forming a bi-layer [(**i**) ½-x, ½-y, -z]

Crystals of $[GunH]_2[Hpzdc]\cdot 2.59H_2O$ (**2**) revealed a strong propensity for twinning with disorder (leading to high residuals, Table 1) but clearly revealed the molecular connectivity and salient packing features. Salt **2** crystallises in the triclinic space group *P-1* and reveals two crystallographically independent $GunH^+$ cations, one pyrazoledicarboxylate di-anion, $Hpzdc^{2-}$ and 2.5 water molecule in the asymmetric unit. Both carboxylic acid groups in the pyrazole-3,5-dicarboxylic acid are now deprotonated with C-O bond lengths (1.253(2) –1.256(2) Å) comparable with those observed for the carboxylate ion within **1**. The C-N bonds in the guanidinium cations span the range 1.307(3)–1.325(3) Å, again consistent with the chemical equivalence of the C-N bonds within the guanidinium cation.

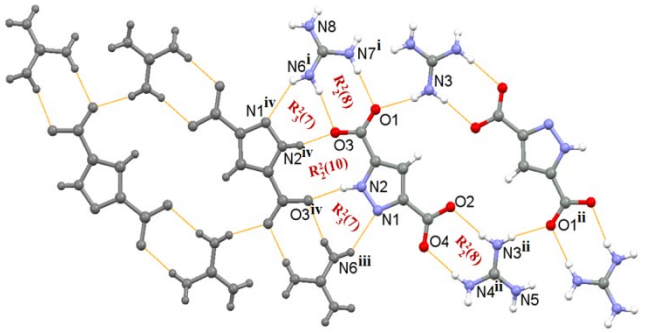

(a)

Each $Hpzdc^{2-}$ dianion forms a pair of N-H…O hydrogen bonds (2.01(2)-2.02(2) Å) to a single cation, such that the two crystallographically independent cations are each doubly hydrogen-bonded to the dianion (Fig. 3a). O1 and O3 are additionally hydrogen bonded to other $[GunH]_2[Hpzdc]$ units via O…H-N contacts to pyrazole and guanidinium units (2.13(2) Å) forming chains of such trimeric units in the *ab* plane (Fig. 3a). The remaining two O atoms (O2 and O4) of the carboxylate form hydrogen-bonded contacts out of the molecular plane to a water molecule (OH…O 2.04(4) Å) and a guanidinium cation (NH…O 2.01(2) Å).

Each of the crystallographically independent $GunH^+$ cations offers 6 hydrogen-bond donor N-H units. $GunH^+$ containing N6 – N8 uses all 6 N-H bonds in in-plane hydrogen bonding; N6 and N7 are involved in a double hydrogen-bond to a carboxylate (discussed above); N7 and N8 are involved in a double hydrogen bond to the pyrazole N and carboxylate O whereas N6 and N8 form hydrogen bonds to the lattice water (N-H…O 2.16(2) and 2.46(2) Å) (Fig. 3b).

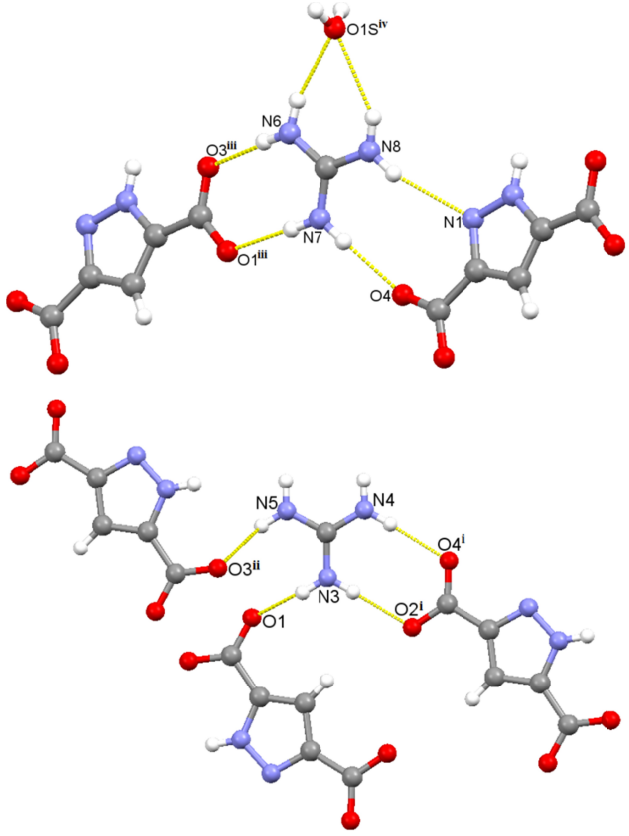

(b)

Fig. 3 (**a**) Crystal packing of **2** highlighting 'in-plane' hydrogen bonds to generate a ribbon-like motif. Two $[GunH]_2[Hpzdc]$ units are highlighted in colour on the right hand side [(**i**) -1+x, 1+y, z; (**ii**) -x, -y, 2-z; (**iii**) 2-x, -y, 1-z; (**iv**) 1-x, 1-y, 1-z]; (**b**) Intermolecular hydrogen bonds to the two crystallographically independent $GunH^+$ cations [(**i**) –x, -y, 2-z; (**ii**) –x, 1-y, 1-z; (**iii**) 1+x, -1+y, z; (**iv**) 1+x, y, -1+z].

The second independent $GunH^+$ cation implements only four of the 6 N-H groups in hydrogen bonding; N3 and N4 forming a double hydrogen bond to the carboxylate anion (see above) while N3 and N5 forming additional hydrogen bonds to two other carboxylate O atoms (N-H…O at 2.13(2) and 2.58(2) Å respectively). Both N4 and N5 each have one N-H bond which is not involved in hydrogen bonding with no close contacts within the sum of the van der Waals radii plus 0.2 Å (Fig. 3b). The hydrogen bonding in **2** can be described as $[GunH]_2[Hpzdc]$ 'trimers' in which the ions are connected by $R^2_2(8)$ rings. Each trimer is joined to a neighboring trimer by 4 hydrogen bonds: an $R^2_2(10)$ ring in the middle, flanked on each side by $R^2_3(7)$ rings. This produces a hexamer which is connected to neighboring hexamers on either side by $R^4_4(20)$ rings forming an infinite ribbon.

Crystals of the 2:1 salt $[AgunH]_2[Hpzdc]\cdot H_2O$ (**4**) were formed from the reaction of aminoguanidine bicarbonate with pyrazole-3,5-dicarboxylic acid in a 2:1 mole ratio. This salt crystallizes in the triclinic space group *P-1* with two $[AgunH]^+$ cations, a pyrazole-3,5-dicarboxylate di-anion, $Hpzdc^{2-}$, and a water molecule in the asymmetric unit (Fig. 1). The guanidinium component of the $AgunH^+$ cation is conjugated with near equivalent C-N bond lengths in the range 1.321(2) – 1.338(2) Å. The conjugated nature of the guanidinium core mitigates against these guanidinium N lone pairs being basic.

Although the hydrazinic N-N bonds lie in the molecular plane, the positions of the H atoms (located in the difference map) indicate the terminal NH_2 groups [N(14) and N(24)] are sp^3-like in character and exhibit some lone pair donor character with one of the two crystallographically independent N-NH_2 groups acting as a hydrogen-bond acceptor (*vide infra*). The C-O bond lengths (1.256(1) – 1.265(2) Å) are consistent with each carboxyl group existing as the carboxylate anion.

The presence of the additional amino group leads to an overall more complex packing motif than that observed for **2** which has the same formal stoichiometry, except water molecules, i.e. $[BaseH]_2[Hpzdc]\cdot H_2O$. In **2**, there is a slight excess of hydrogen bond donors [13 N-H and 2 O-H groups] in relation to the eleven potential H-bond acceptors [10 O lone pairs and one N lone pair on the $Hpzdc^{2-}$ dianion]. In **4**, the 17 hydrogen bond donors [7 per $AgunH^+$ plus 2 H_2O H-bond donors plus the $Hpzdc^{2-}$ N-H bond] can only be partially fulfilled by the anion and solvent water molecules [8 O lone pairs per di-anion, 2 lone pairs per water-O, the N lone pair of the di-anion and a lone pair per terminal $AgunH^+$ amine group = 13 E-H bond acceptors].

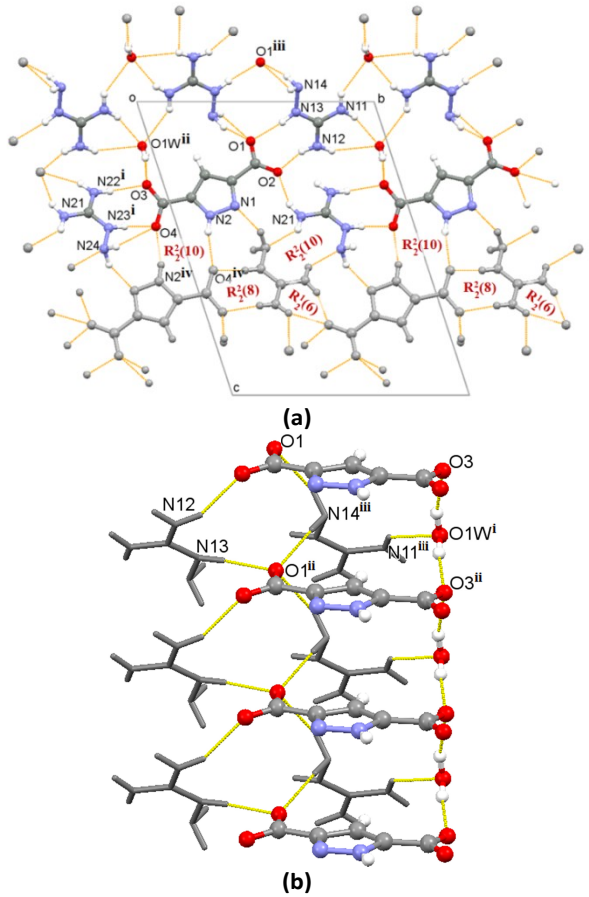

Fig. 4 (**a**) Packing of **4** in the ***bc***-plane (one molecular tape is highlighted in colour, the second in grey) [(i) x, -1+y, z; (ii) 1+x, -1+y, z; (iii) 1-x, 1-y, -z; (iv) 1-x, -y, 1-z] and (**b**) view of water molecule and π-π stacking between adjacent $Hpzdc^{2-}$ anions [(**i**) x, -1+y, z; (**ii**) -1+x, y, z; (**iii**) -x, 1-y, -z].

In **4**, a complex hydrogen-bonding network forms a layer-like structure in the *bc* plane (Fig. 4a). Hydrogen bonding between the $Hpzdc^{2-}$ di-anion and one of the two crystallographically unique $AgunH^+$ cations (containing N21) generates a hydrogen-bonded chain parallel to the crystallographic *b*-axis. The carboxylate O(3) and O(4) atoms form a pair of hydrogen bonds to N(22) and N(23) (1.96(1) – 1.98(1) Å), whereas O(2) forms an N-H…O contact to N(21) (1.92 Å) (Table 2). Another chain comprising the second $AgunH^+$ cation propagates parallel to this chain with $AgunH^+$ cations bridged by O atoms; two lattice solvent molecules (O1W) each form a pair of N-H…O contacts (2.16(1) – 2.31(1) Å) to N(11) atoms located around an inversion centre. In addition the $Hpzdc^{2-}$ carboxylate O1 takes up a similar role doubly bridging between N(13) and N(14) (N-H…O at 1.91(1) and 2.04(1) Å). Additional hydrogen bonding between the pyrazolle N-H and carboxylate O(4) (1.99(1) Å) further links these chains in the *bc* plane.

Between these layers the dianions stack parallel to the crystallographic *a*-axis. The face-to-face, π-π stacking interaction between the two planar pyrazole $Hpzdc^{2-}$, heterocycles (centroid…centroid distance = 3.997 Å) is substantially longer than the inter-layer contacts in graphite (3.35 Å) and this stacked motif appears to arise from a complex hydrogen-bonded network in which anions are held together *via* bridging $AgunH^+$ units and water molecules (Fig. 4b): The water molecule forms two O-H…O hydrogen bonds between di-anions with O…H contacts of 1.88(1) and 2.06(1) Å. In addition the amine N(14) forms two N-H…O hydrogen bonds to O1 (2.04(1) and 2.49(1) Å). A third bridge is formed by another $AgunH^+$ cation with N(12)-H…O(2) at 2.09(1) Å and N(13)-H…O(1) at 1.91(1) Å. The hydrogen bonding in **4** can be described as pairs of antiparallel $([AgunH][[Hpzdc])^-_n$ chains in which $AgunH^+$ and $Hpzdc^{2-}$ molecules are connected alternatively by $R^2_2(8)$ rings (as seen in structure **2**) and $R^1_2(6)$ rings. These neighboring pairs of chains are connected to each other by $AgunH^+$ ions in $R^2_2(10)$ rings generating an overall 2D network.

Compound **9**, [TagunH][H_2pzdc][H_3pzdc], also crystallises in the triclinic space group *P-1* with one $TagunH^+$ cation, one H_2pzdc^- mono-anion and one neutral H_3pzdc molecule in the asymmetric unit. The C-O bond lengths for the carboxylic acid groups clearly comprise the expected long C-O (1.283(17)-1.292(17) Å) and short C=O (1.221(17)-1.241(18) Å) bond lengths. The fourth carboxylate anion has more similar geometric parameters with C1-O2 and C1-O1 at 1.240(17) and 1.268(17) Å respectively. As with $AgunH^+$, the $TagunH^+$ is planar with the NH_2 groups rotated out of the ring plane. The change in stoichiometry to 1:2 now provides sufficient hydrogen bond acceptors for every N-H group with 14 H-bond donors and 18 potential H-bond acceptors.

The mono-deprotonated and free pyrazole-3,5-dicarboxylic acids form a hydrogen-bonded chain parallel to the [011] direction (Fig. 5a). This hydrogen-bonded chain comprises a classical carboxylic acid dimer between two COOH groups of the neutral H_3pzdc with the remaining two COOH groups forming a further hydrogen bond to the COO^- group of the H_2pzdc^- anion. The O-H…O hydrogen bonded distances fall in the range 1.53(4) – 1.65(3) Å. The O(2) atom of the carboxylate anion and O(7) of the parent acid are both involved in inter-chain hydrogen bonding to the pyrazole N-H groups (N-H…O at 1.90(19) and 1.96(19) Å), leading to a two-dimensional network (Fig. 5a).

The TagunH$^+$ offers a total of 9 N-H hydrogen bond donors; three in the plane of the TagunH$^+$ cation and 6 oriented out of the molecular plane. Two of the in-plane N-H groups form N-H…N hydrogen bonds to other TagunH$^+$ cations in the range 2.11(2) – 2.63(2) Å forming hydrogen-bonded chains (Fig. 5b). These chains of cations interpenetrate the two-dimensional layer of $[H_3pzdc][H_2pzdc]^-$ forming a complex three dimensional network (Fig. 5c) with N-H…O and N-H…N hydrogen bonds between cationic threads and anionic layers in the range 2.11(2)-2.25(11) Å). In crystal packing, the different type of hydrogen bonds to generate an infinite 3D hydrogen-bonded network that further sustained *via* π-π stacking, various π-interactions (N-H…π, C-O…π, C-OH…π & COOH-π) and strong O-H…O hydrogen bonding in the ABAB manner (Fig. 5d).

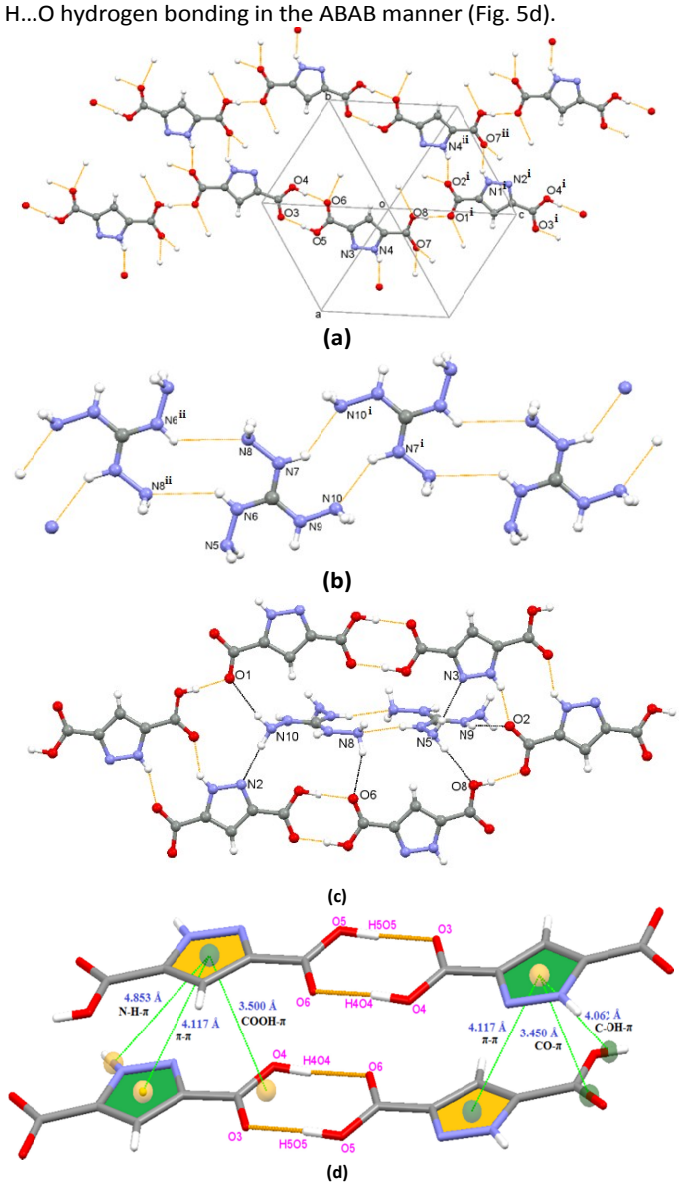

Fig. 5 (a) View of compound **9** revealing hydrogen bonding network between H_2pzdc^- and H_3pzdc [(i) -1+x, -1+y, 1+z; (ii) -1+x, y, z]; (**b**) H-bonded interactions between the TagunH$^+$ cations [(i) 1-x, 2-y, 2-z; (ii) 1-x, 2-y, 1-z]; (**c**) interpenetration of TagunH$^+$ threads within the 2D anionic network, (**d**) The various type of inter-molecular forces between adjacent H_2pzdc^- anions and free H_3pzdc

Discussion

The propensity of the H_2pzdc^- anion to form N-H…O hydrogen bonds is reflected in the structure of **1** in which the N-H…O hydrogen bonds common to **2**, **4** and **9** are replaced by an alternative set of N-H…O contacts; one to the lattice water and the other to the GunH$^+$ cation. Thus these structures appear to attempt to satisfy, to a large degree, the extensive hydrogen-bonding capacity of both cation and anion. The propensity of the H_2pzc^- anion to involve the N-H donor and carboxylate-O as hydrogen-bond acceptor with the formation of a complimentary pair of N-H…O hydrogen bonds is reflected in the structures of **1**, **2**, **4** and **9** (Fig. 6).

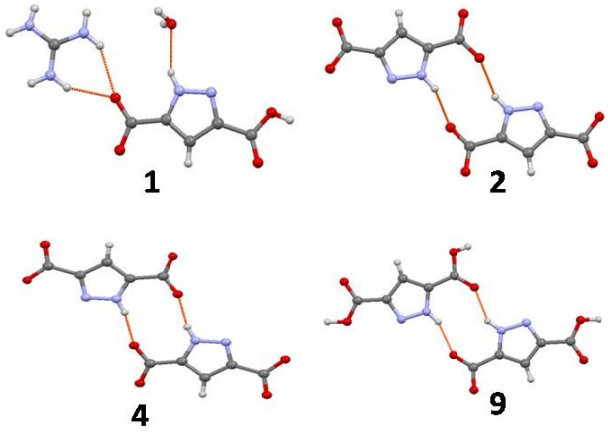

Fig. 6 Hydrogen bonding in **1**, **2**, **4** and **9**

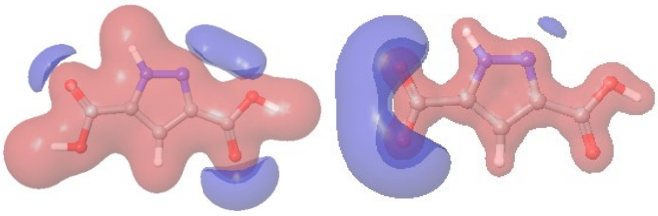

Fig. 7 Molecular electrostatic iso-potentials for H_3pzdc (left) and H_2pzdc^-(right) (surfaces plotted at 25 kJ/mol and 120 kJ/mol, respectively)

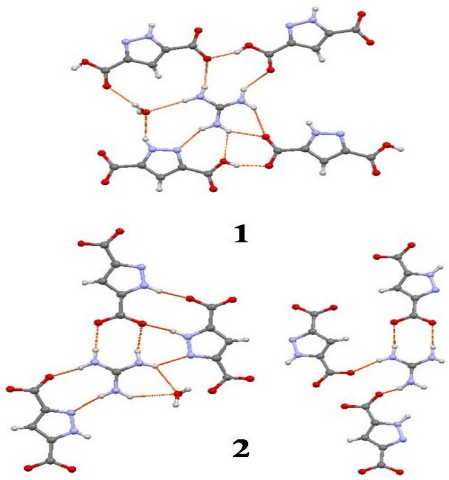

Fig.8 Hydrogen-bonded contacts to the GunH$^+$ cation in **1** (top) and the two crystallographically independent GunH$^+$ cations in **2** (bottom)

Table 1 Crystallographic data for compounds **1**, **2**, **4** and **9**

Compounds	**1**	**2**	**4**	**9**
Empirical formula	$C_6H_{11}N_5O_5$	$C_7H_{19.16}N_8O_{6.59}$	$C_7H_{18}N_{10}O_5$	$C_{11}H_{16}N_{10}O_8$
Formula weight	233.20	320.83	322.31	416.34
Temperature/K	296(2)	296(2)	173(2)	296(2)
Crystal system	Monoclinic	Triclinic	Triclinic	Triclinic
Space group	*C2/c*	*P-1*	*P-1*	*P-1*
a/Å	12.7602(4)	7.7868(14)	3.9966(2)	8.7785(4)
b/Å	9.0277(4)	10.0032(18)	12.0312(6)	9.7547(4)
c/Å	17.1544(7)	10.6058(19)	15.5723(9)	10.2957(5)
α/°	90	72.744(6)	71.941(2)	93.527(2)
β/°	95.503(3)	70.282(6)	89.275(2)	101.291(2)
γ/°	90	75.842(6)	84.754(2)	102.406(2)
Volume/Å^3	1967.00(13)	733.0(2)	708.81(7)	839.43(7)
Z	8	2	2	2
ρ_{calc}g/cm^3	1.575	1.454	1.510	1.647
μ/mm^{-1}	0.137	0.126	0.127	0.141
F(000)	976	332	340	432
Crystal size/mm^3	0.30 × 0.20 × 0.20	0.35 × 0.30 × 0.30	0.70 × 0.30 × 0.07	0.40 × 0.35 × 0.30
Radiation	Mo-Kα (λ = 0.71073)	Mo-Kα (λ = 0.71073)	Mo-Kα (λ = 0.71073)	Mo-Kα (λ = 0.71073)
2θ range for data collection	5.54 to 56.62°	4.32 to 56.26°	6.82 to 61.10°	5.58 to 56.46°
	-13 ≤ *h* ≤ 16	-10 ≤ *h* ≤ 9	-5 ≤ *h* ≤ 5	-11 ≤ *h* ≤ 11
Index ranges	-11 ≤ *k* ≤ 11	-12 ≤ *k* ≤ 13	-17 ≤ *k* ≤ 17	-11 ≤ *k* ≤ 12
	-20 ≤ *l* ≤ 22	-14 ≤ *l* ≤ 11	-22 ≤ *l* ≤ 22	-11 ≤ *l* ≤ 13
Reflections collected	7327	3555	29616	5492
Independent reflections	2410	2522	4324	3221
R_{int}, R_σ	0.0163, 0.0166	0.0253, 0.0516	0.0573, 0.0322	0.0150, 0.0242
Data/restraints/parameters	2410/10/175	3327/15/221	4324/16/258	3941/3/318
Goodness-of-fit on F^2	1.033	1.055	0.990	1.059
Final R indexes [*I*>2σ(*I*)]	R_1 = 0.0342, wR_2 = 0.0955	R_1 = 0.0431, wR_2 = 0.1234	R_1 = 0.0413, wR_2 = 0.1095	R_1 = 0.0373,wR_2 = 0.1066
	R_1 = 0.0392,	R_1 = 0.0559,	R_1 = 0.0532,	R_1 = 0.0437,
Final R indexes[all data]	wR_2 = 0.0996	wR_2 = 0.1322	wR_2 = 0.1196	wR_2 = 0.1137
Largest difference peak/hole / e Å^{-3}	+0.37/-0.21	+0.18/-0.20	+0.47/-0.27	+0.29/-0.27

DFT calculations (B3LYP/6-311G*) of both H_3pzdc[80,81] and H_2pzdc$^-$ were undertaken in order to probe the molecular electrostatic potential (MEP) surfaces. These reveal for neutral H_3pzdc regions the expected negative charge (blue) around the carbonyl O atoms (proton acceptor) and a combined region of negative charge arising between the carboxylic acid and the pyrazole N-donor atom (Fig. 7). Conversely there is a build-up of positive charge (red) associated with the two carboxylic acid protons and, to a lesser extent the pyrazole N-H. Deprotonation leads to major redistribution of charge in the MEP, reflected in substantially larger energy terms, coupled to strong polarisation of negative charge in the vicinity of the carboxylate anion. Contacts between cation N-H and neutral H_3pzdc now favour short contacts to carboxylic acid C=O groups and a bifurcated interaction to the N/O combination associated with the pyrazole and carboxylic acid groups. Deprotonation will lead to dominant interactions to the deprotonated carboxylate group. An examination of the close contacts to the GunH$^+$ cation (Fig. 8) reflects all these types of favourable contact.

Powder X-ray diffraction studies

Powder X-ray diffraction (PXRD) and single-crystal X-ray diffraction (SCXRD) are the two general methods of X-ray diffraction applications. Powder XRD is the major method for crystallographic characterization for bulk materials. It is a powerful and quick technique for identification of the homogeneous and single phase unknown materials. PXRD is usually used as the fast identification of polymorphs or polymorphic mixture while single-crystal X-ray diffraction determines the detailed crystal structures as well as molecular conformation. The powder XRD patterns of the synthesized samples (Experimental and simulated PXRD) are presented in Fig. 9, the sharp lines and slightly differ in peak position/intensity of the 2θ values indicating an overall crystalline and polymorphic nature of the products. Further, the experimental PXRD patterns for **1**, **2**, **4** and **9** are in very close agreement to the corresponding derived patterns from the single crystal data which clearly indicate that all salts are different polymorphs, and crystalline in nature (simulated PXRD derived from SCXRD) as shown in Fig. 9. The remaining experimental PXRD data's are provided in the supplementary information (Figs. 5-9, ESI).

Table 2 Hydrogen bonding for the compounds **1, 2, 4** & **9**

1				
D-H...A	D-H	H...A	D-H...A (Å)	D-H...A (°)
O1S-H1SA...O3^{i}	0.86(15)	2.10(16)	2.917(13)	158(18)
O1S-H1SB...O4^{ii}	0.86(14)	2.00(15)	2.865(15)	178(19)
O1-H1...O2^{iii}	0.91(14)	1.64(15)	2.539(11)	168(17)
N5-H5A...O1S^{iv}	0.89(14)	2.27(14)	3.157(17)	177(15)
N5-H5B...O2^{v}	0.87(14)	2.07(14)	2.934(14)	178(16)
N3-H3A...N2^{iv}	0.86(14)	2.12(15)	2.933(14)	158(17)
N3-H3B...O4^{ii}	0.87(14)	2.09(15)	2.901(14)	155(17)
N1-H1A...O1S	0.86(13)	2.11(14)	2.889(14)	151(13)
N4-H4A...O3^{vi}	0.83(14)	2.14(16)	2.862(13)	145(17)
N4-H4B...O4^{ii}	0.86(14)	2.31(15)	3.059(15)	146(15)
Symmetry code:(i) x, 1-y, -1/2+z (ii) 1/2-x, 1/2-y, -z (iii) x, 1+y, z (iv) 1/2-x, 3/2-y, -z (v) 1/2-x, 1/2+y, 1/2-z (vi) 1/2-x, -1/2+y, 1/2-z				

2				
D-H...A	D-H	H...A	D-H...A(Å)	D-H...A (°)
N2-H2...O3^{i}	0.86	2.13	2.89(2)	147
N3-H3A...O2^{ii}	0.86	2.01	2.87(2)	176
N3-H3B...O1	0.86	2.13	2.90(2)	148
N4-H4A...O4^{ii}	0.86	2.02	2.88(2)	177
N4-H4B...O0AA	0.86	2.09	2.93(18)	164
N4-H4B...O2AA^{iii}	0.86	2.44	3.19(7)	146
N5-H5A...O1AA	0.86	2.10	2.99(6)	165
N5-H5A...O2AA^{iii}	0.86	2.22	3.02(8)	155
N5-H5B...O3^{iv}	0.86	2.58	3.14(3)	124
O1S-H1SA...O2	0.85(3)	2.04(4)	2.80(3)	149(4)
Symmetry code: (i) 1-x, 1-y, 1-z (ii) -x, -y, 2-z (iii) -2-x, 1-y, 2-z (iv) -x, 1-y, 1-z				

4				
N2-H2...O4^{i}	0.87(1)	1.99(1)	2.841(1)	165(1)
N13-H13...O1^{ii}	0.87(1)	1.91(1)	2.772(1)	172(1)
N11-H11A...O1w^{iii}	0.86(1)	2.31(1)	3.010(1)	138(1)
N14-H14A...O1^{iv}	0.91(1)	2.04(1)	2.915(1)	162(1)
O1w-H1w...O3^{v}	0.87(1)	1.88(1)	2.740(1)	172(1)
O1w-H2w...O3^{vi}	0.86(1)	2.06(1)	2.881(1)	160(1)
N22-H22A...O3^{vi}	0.87(1)	1.98(1)	2.842(1)	171(1)
N21-H21B...N24^{vii}	0.86(1)	2.22(1)	2.954(1)	142(1)
N23-H23...O4^{vi}	0.87(1)	1.96(1)	2.820(1)	169(1)
N24-H24B...N1^{viii}	0.93(1)	2.24(1)	3.106(2)	156(1)
Symmetry code: (i) 1-x, -y, 1-z (ii) 1-x, y, z (iii) -x, 2-y, -z (iv) 1-x, 1-y, -z (v) -1+x, 1+y, z (vi) x, 1+y, z (vii) –x, 1-y, 1-z (viii) 1-x, 1-y, 1-z				

9				
O8-H8...O1^{i}	1.11(2)	1.36(2)	2.475(14)	179(17)
N1-H1...O7^{iii}	0.89(19)	1.90(19)	2.750(16)	159(17)
N5-H5B...N3^{iv}	0.86(9)	2.25(11)	3.073(18)	161(17)
N9-H9...O2^{i}	0.90(2)	2.09(2)	2.907(17)	150(17)
N7-H7...N10^{v}	1.01(2)	2.24(2)	3.097(2)	142(18)
N10-H10A...N2^{ii}	0.95(2)	2.11(2)	3.059(18)	177(16)
N10-H10B...O1^{vi}	0.88(2)	2.25(2)	3.108(17)	167(17)
N4-H4...O2^{vii}	0.84(19)	1.96(19)	2.760(16)	159(18)
O4-H4A...O6	0.97(3)	1.65(3)	2.613(14)	176(3)
O5-H5...O3	1.07(4)	1.53(4)	2.599(15)	177(3)
Symmetry code: (i) -1+x, -1+y, 1+z (ii) 1-x, 2-y, 1-z (iii) x, 1+y, -1+z (iv) -1+x, y, z (v) 1-x, 2-y, 2-z (vi) 2-x, 2-y, 1-z (vii) x, -1+y, 1+z				

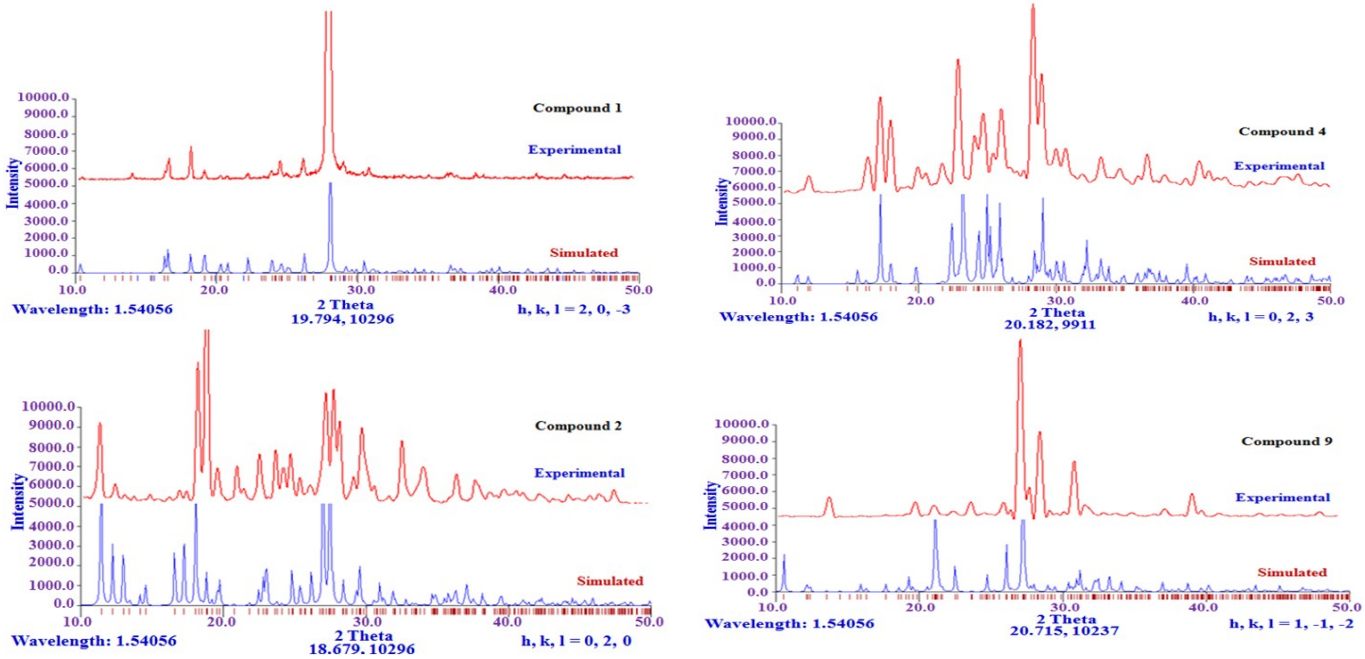

Fig. 9 Experimental and simulated (derived from single crystal XRD) PXRD patterns of compounds **1, 2, 4** & **9** are shown for comparison

Table 3 Thermal studies free acid (H_3pzdc) and its salts **1 – 9**

Compound		DTA Peak Temp./°C	Thermogravimetry			Decomposition products
			Temp. range/°C	Mass loss/%		
				Obsd.	Calcd.	
$H_3pzdc.H_2O$		(+) 110	80-130	10.30	10.35	H_3pzdc
		(+) 300	250-600	100	100	Gaseous products
$[GunH][H_2pzdc].H_2O$	**1**	(+) 180	110-200	7.60	7.77	$[GunH][H_2pzdc]$
		(+) 270	-	-	-	Melting
		(+) 290	250-300	39.80	39.87	H_3pzdc
		(+) 345	300-350	58.90	58.74	Pyrazole-3-carboxylic acid
		(-) 530	350-600	100	100	Gaseous products
$[GunH]_2[Hpzdc].2.59H_2O$	**2**	(+) 135 (+) 155	100-230	13.10	14.22	$[GunH]_2[Hpzdc]$
		(+) 245	-	-	-	Melting
		(+) 290	250-400	52.00	51.00	H_3pzdc
		(-) 590	400-600	100	100	Gaseous products
$[AgunH][H_2pzdc].H_2O$	**3**	(+) 240	200-250	7.20	7.28	$[AgunH][H_2pzdc]$
		(+) 280	250-300	13.40	13.36	$[GunH][H_2pzdc]$
		(-) 375 (-) 420	300-400	37.65	37.65	H_3pzdc
		(-) 475 (-) 500	400-620	100	100	Gaseous products
$[AgunH]_2[Hpzdc].H_2O$	**4**	(+) 120	100-180	5.50	5.58	$[AgunH]_2[Hpzdc]$
		(+) 140	-	-	-	Melting
		(+) 190 (-) 265	200 – 380	52.20	52.12	H_3pzdc
		(-) 545	380-600	100	100	Gaseous products
$[AgunH][H_2pzdc][H_3pzdc]$	**5**	(+) 275	200-280	19.60	19.58	2 moles of H_3pzdc
		(-) 370 (-) 410	280-450	59.80	59.79	H_3pzdc
		(-) 485	450-610	100	100	Gaseous products
$[DagunH][H_2pzdc].H_2O$	**6**	(+) 115	-	-	-	Melting
		(+) 170 (+) 270	100-300	41.20	41.23	H_3pzdc
		(-) 580	300-600	100	100	Gaseous products
$[DagunH]_2[Hpzdc].H_2O$	**7**	(+) 60	40-100	5.00	5.10	$[DagunH]_2[Hpzdc]$
		(+) 180	-	-	-	Melting
		(+) 260 (+) 300	200-300	81.15	81.24	Pyrazole
		(-) 495 (-) 525	330-600	100	100	Gaseous products
$[DagunH][H_2pzdc][H_3pzdc]$	**8**	(+) 175	-	-	-	Melting
		(+) 210	100-250	22.50	22.64	2 moles of H_3pzdc
		(-) 300 (-) 600	250-630	100	100	gaseous products
$[TagunH][H_2pzdc][H_3pzdc]$	**9**	(+) 245	-	-	-	Melting
		(+) 270	200-250	25.20	25.44	2 moles of H_3pzdc
		(+) 350	250-440	62.50	62.72	H_3pzdc
		(-) 500 (-) 575	440-600	100	100	gaseous products

[(+) = endothermic; (-) = exothermic]

Thermal decomposition studies

In order to compare the thermal stability of the salts, simultaneous TG-DTA is carried out from room temperature to 800°C. The mono- and bis-guanidinium salts are hydrated whereas the acid-rich salts, which offer sufficient hydrogen-bond acceptors to satisfy the number of N-H bond donors offered by the base, are anhydrous (Table 3). The endotherms for freshly prepared samples reveal water evolution from the 1:1 and 2:1 salts **2**, **4**, **6** and **7** at 135, 120, 115 and 60°C, respectively in DTA, whereas dehydration of isolated salts **1** and **3** occur at 180 and 240°C, respectively. This suggests that the water molecules in both **1** and **3** are an integral part of the crystal structure.[56,82] The TG plots revealed weight loss equivalent to a single water molecule per salts/crystal in all cases consistent with the micro-analytical data and, where available, the crystallographic data. The TG curves are given in Fig. 10, as representative examples, whilst remaining data are provided in the electronic supplementary information (ESI, Figs. S10-15). The water-free, acid-rich 1:2 salts reveal enhanced stability with the onset of an endothermic decomposition at 250°C.

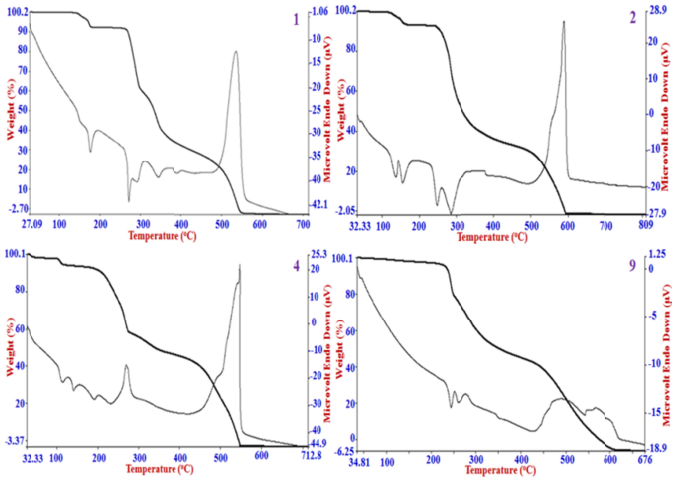

Fig.10 Simultaneous TG/DTA of [GunH][H_2pzdc].H_2O, (**1**) [GunH]$_2$[Hpzdc].2.5H_2O, (**2**) [AgunH]$_2$[Hpzdc].H_2O (**4**) and [TagunH][H_2pzdc][H_3pzdc] (**9**).

Fluorescence Studies

The pyrazole-3,5-dicarboxylic acid(H_3pdc) is an attractive ligand for studies of energy transfer because of its conjugation within the pyrazole ring. In our present study, we found that the free acid and its prepared salts exhibit photoluminescence in solid state. The free acid exhibits a weak emission peak at 373 nm upon excitation at 330 nm. This is analogous to the isomer of pyrazole-3,4-dicarboxylic acid which also exhibits similar emission characteristics.[83]

The enhancement and the blue/red shift of the luminescence of the pyrazole-3,5-dicarboxylate ligand compared to that of free acid may, therefore, be attributed to the deprotonation of the carboxylic group (Fig. 11). This effectively enhances the rigidity of the ligand and reduces the loss of energy by radiation less decay of the intra ligand emission of the excited state. In addition, fluorescent emission of free ligands resulting from the π*-*n* transition is very weak compared with that of the π*-π transition of the pyrazole-3,5-dicarboxylate ion. As can be seen, the main emission bands of all the salts are located almost at the same position and exhibit a red shift, which has been attributed to the π*-π transition of the carboxylate ligand. The differences in the band shape might also be due to the minor differences in the structural topologies. As a whole, these salts exhibit relatively strong emission bands at room temperature, indicating they may be good candidates for photoactive materials.

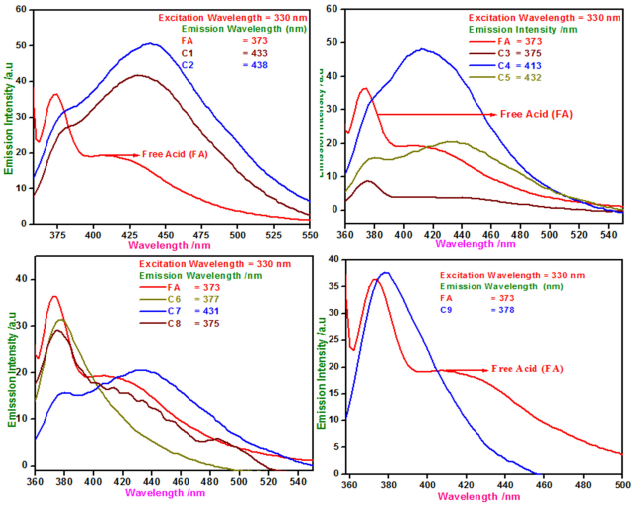

Fig. 11 Emission spectra of free acid and its salts [FA = free acid; C1…C9 refer to compounds **1 – 9**]

Antibacterial activity

The disc diffusion assay was conducted to determine[84-88] the minimum inhibitory concentration (MIC), is the least concentration of the test compounds which inhibit the growth of bacteria. The antibacterial activity of the free acid and its prepared salts (**1-9**) has been screened against the gram positive (*Bacillus substilis, Staphylococcus aureus & Staphylococcus albush*) and gram negative (*Salmonella paratyphi, Escherichia coli & Klebsella pneumoniae*) bacteria. Significant antibacterial activities were observed for salts **1-9** and free acid when compared to a standard drug *Ciprofloxacin* and 10%DMSO was used as a control. Among all the nine guanidinic salts and free acid tested, the salts of **4**, **7** and **9** exhibited comparable activity against the entire six pathogenic microorganisms than other salts. Data obtained also indicate the increasing dosage level of compounds, the inhibitory effect was increased. The minimum inhibitory concentrations (MIC) are given in Table 4. Salt **9** revealed superior inhibitory effects against *B. substilis, S. Aureus* and *E. Coli* with MIC values around or between 25-35 μg mL^{-1}. The other salts **1, 2, 3** and **6** showed relatively less (MIC ≤ 300 μg mL^{-1}) inhibitory effect than bis- and acid rich salts. The salts **5** and **8** showed moderate activities against the tested bacterial pathogens. It is worthwhile to mention here that the antibacterial activity increases as the number of hydrazine moieties increases. Hence it is evident that the di-salts showed a greater area of inhibition than those of mono-salts and free acid. Accordingly, the activity seems to correlate strongly with the number of

hydrazine moieties present and is consistent with previous studies.[87,88]

Table 4 The range of inhibitory concentration (MIC) values of the free acid (FA)[a] and its salts **1–9**[a]

Compounds	Minimum inhibitory concentration (μg mL^{-1})					
	B. substilis	*S. aureus*	*S. albush*	*S. paratyphi*	*E. coli*	*K. pneumoniae*
Free acid	---	---	---	---	>300	---
1	250	300	---	---	200	---
2	200	150	>250	---	>150	---
3	150	>150	200	200	<150	250
4	**100**	**90**	**>150**	**95**	**80**	**80**
5	100	100	150	<150	100	150
6	<150	100	200	100	150	200
7	**80**	**75**	**80**	**65**	**70**	**90**
8	<150	100	150	100	<150	100
9	**25**	**35**	**60**	**50**	**20**	**45**
Ciprofloxacin	**25**	**30**	**20**	**20**	**15**	**25**
Control	NI	NI	NI	NI	NI	NI

[a]NI: No inhibition; "> or <" above or below the (MIC) activities; values in red – standard, and in green – relatively more active in present study; '---' means no active

Antioxidant activity

The total antioxidant and DPPH scavenging activity of the free acid, H_3pzdc, and its salts of different concentration have been determined and are presented in Figs. 12 and 13. As per the Bondet *et al*[89] model, it appears that there are three possible pathways for base (e.g. Agun)/DPPH$^{\bullet}$ reactions that are shown in Scheme 3. In the first step (a), the Agun moiety is transformed into Agun$^{\bullet}$ by donation of H-atom. In the next step (b), two parts of Agun$^{\bullet}$ combine to form a dimerized product (bis-aminoguanidine). The third pathway (c), involves a complexation between Agun$^{\bullet}$ and DPPH$^{\bullet}$. From the reaction sequence, it is clear that two species of Agun are required for dimerization leading to better scavenging activity. Further, it is evident from the results that the total antioxidant activity can be attributed to the increasing number of amine groups appended to the guanidine core. Thus the following order of total antioxidant and DPPH scavenging activity was obtained: H_3pzdc<GunH$^+$<AgunH$^+$<DagunH$^+$<TagunH$^+$. The triamino-guanidinium derivative **9** appears to have the highest total antioxidant activity among all the salts studied. It is clearly observed that increasing the addition of one NH_2 group in guanidine moiety facilitates the total antioxidant capacity (TAC) as shown in Fig. 12. Notably increasing the number of amine functionalities increases the DPPH scavenging activity. Thus the free acid and guanidinium salts **1** and **2** have low activity (Fig. 13). Conversely, the compounds **3**-**5** were significantly more active with **4** (where the ratio of Agun:H_3pzdc= 2:1) exhibiting higher activity than both **3** and **5** (1:1 ratio). Similar trends are observed for the DagunH$^+$ derivatives which exhibit higher activity than AgunH$^+$ and highest activity when the DagunH$^+$:H_3pzdc ratio is 2:1. Finally TagunH$^+$ with three hydrazine functionalities exhibits the highest activity. Thus the activity seems to correlate strongly with the number of hydrazine moieties present and is

amine functionalities increases the DPPH scavenging activity. Thus the free acid and guanidinium salts **1** and **2** have low activity (Fig. 12). Conversely, the compounds **3**-**5** were significantly more active with **4** (where the ratio of Agun:H_3pzdc= 2:1) exhibiting higher activity than both **3** and **5** (1:1 ratio). Similar trends are observed for the DagunH$^+$ derivatives which exhibit higher activity than AgunH$^+$ and highest activity when the DagunH$^+$:H_3pzdc ratio is 2:1. Finally TagunH$^+$ with three hydrazine functionalities exhibits the highest activity. Thus the activity seems to correlate strongly with the number of hydrazine moieties present and is further consistent with previous studies which reveal that hydrazine derivatives are well-established as antioxidants.[90,91]

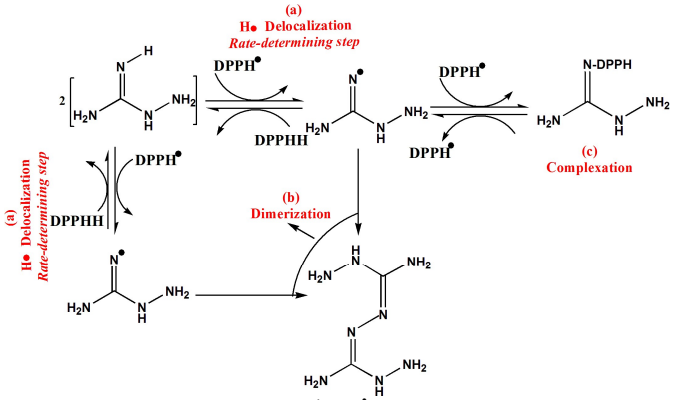

Scheme 3 Proposed mechanism for Agun/DPPH$^{\bullet}$ reaction

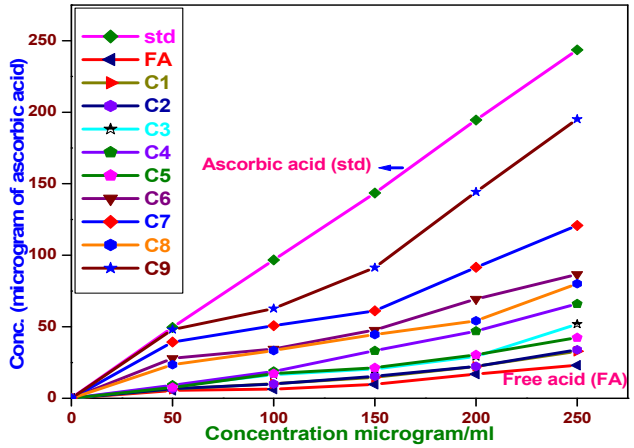

Fig. 12 Total Antioxidant activity of the free acid (FA) and compounds **1** -**9** (labelled C1 – C9)

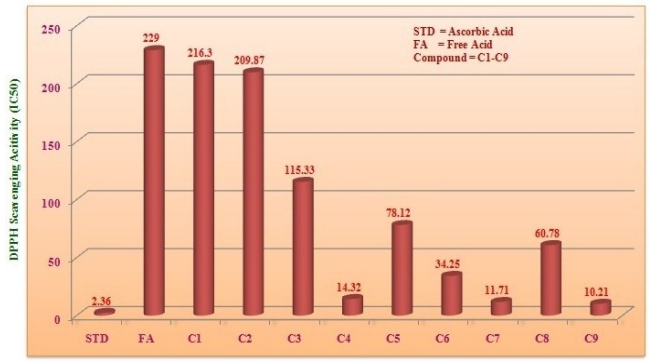

Fig. 13 DPPH radical scavenging activity of the free acid (FA) and compounds **1**-**9** (labelled C1- C9)

Conclusions

The systematic investigation of pyrazole-3,5-dicarboxylic acid with guanidine bases *via* guanidine carbonate, aminoguanidine bicarbonate, diaminoguanidine- and triaminoguanidine-hydrochloride in different mole ratios has yielded three types of salts, *viz.*1:1 salts containing the H_2pzdc^- anion, 2:1 salts containing the $Hpzdc^{2-}$ anion and the acid-rich 1:2 salt containing both H_2pzdc^- and neutral H_3pzdc. The unusual formation of such co-crystals would indicate some stability of [BaseH][H_2pzdc][H_3pzdc] over [BaseH][H_2pzdc] and [H_3pzdc]. The origin of this stability might lie with the large number of NH hydrogen-bond donors associated with the $BaseH^+$ cations which require additional hydrogen bond acceptor groups which are afforded by the presence of additional H_3pzdc. From the structural results, in the formation of mono- and acid-rich salts, it is apparent that the deprotonation takes place invariably in the carboxyl group present in the fifth position of the pyrazole ring than the third. This is probably due to the zwitterionic nature of the latter (pk_a> 3.84). Similar kind of salt formation of H_3pzdc has also been observed with ammonia[76] and hydrazine.[77] From the thermal analysis all the salts undergo dehydration endothermically and oxidative decomposition exothermically to give the acid intermediates. This is somewhat similar to the observation of already reported hetero-aromatic dicarboxylic acids.[56] The necessity to try and meet the hydrogen bonding capacity of such ultra-rich N-H hydrogen bond donors appears to lead to new and unusual structures. In terms of properties we note that the emission spectra of the parent acids have poorer luminescent activity than the salts, whilst the antibacterial and antioxidant properties is in the order $TagunH^+$>$DagunH^+$>$AgunH^+$>$GunH^+$>H_3pzdc and consistent with the presence of hydrazine functionalities as the dominant antibacterial and antioxidant activities. Altogether, it is believed that, the information obtained from the present review would be ultimately helpful to develop new potent water soluble guanidinic salts with effective antibacterial and antioxidant activities. Further studies are underway in our laboratory.

Acknowledgments

The authors (S.P, A.P and S.G) thank the UGC-SAP-DRS II, New Delhi (India) for financial support. S.G. is also thankful for the award of UGC-Emeritus Fellowship by UGC, New Delhi, India and J.M.R. would like to thank the CRC program for financial support. The authors sincerely thank Prof. Horst Puschmann, Durham University, Durham, UK, for the crystallographically assistance in the refinement of compounds **1**, **2** & **9** with recent version of SHELXL-2014/7.

References

1 S. Beatriz, P. Costa, O. E. Piro, R. P. Diez, E. E. Castellano and A. C. Gonzalez-Baro, *Polyhedron,* 2006, **25,** 2920.
2 R. J. Sension, B. Hudson and P. R. Callis, *J. Phys. Chem.,* 1990, **94,** 4015.
3 E. A. Nadia, El-Gamel, J. Wagler and E. Kroke, *J. Mol. Struct.* 2008, **888,** 204.
4 M. J. Bushiri,C. J. Antony and M. Fleck, *J. Raman Spectrosc.,* 2008, **39,** 368.
5 G. Carver, D. Spichiger and P. L. W. Tregenna-Piggott, *J. Chem. Phys.,* 2005, **122,** 124511.
6 Denise,M. Perreault, A. Larry Cabell, Eric and V. Anslyn, *Bioorg. Med. Chem.,* 1997, **5,** 1209.
7 C. J. Antonya, M. JunaidBushirib, H. T. Varghesed, C.Y. Panicker and M. Flecke, *Spectrochim. Acta.,* 2009,**73,** 942.
8 I. Nemec, Z. Machackova, K. Teubner, I. Cisarova, P. Vanek and Z. Micka, *J. Solid State Chem.* 2004, **177,** 4655.
9 M. Gobel and T. M. Klapotke, *Z Anorg Allg Chem.* 2007, **633,** 1006.
10 H. Gao, Y. Huang, C. Ye, B. Twamley and J. M. Shreeve, *Chem. Eur. J.* 2008, **14,** 5596.
11 T. M. Klapotke and J. Stierstorfer, *Cent. Eur. J. Energ. Mater.*2008,**5,** 13.
12 P. P. Deyn(Ed), Guanidino Compounds in Biology and Medicine. London, England: J. Libbey, 1992.
13 O. Krocher, M. Elsener and E. Jacob, NeueReduktionsmittelfür die Low NOx-SCRTechnik/New reducing agents for the low-NOx SCR technology, 5thInternational Exhaust Gas and Particulate Emissions Forum, Ludwigsburg, Germany, 2008.
14 O. Krocher, M. Elsener and E. Jacob, *Appl. Catal.* 2009,**B88,**66.
15 D. J. Haas, D. R. Harris andH. H. Mills, *Acta Crystallogr.*1965,**19,**676.
16 J. M. Adams and R. W. H. Small, *Acta Crystallogr.*1976,**B32,** 832.
17 M. Drozd and J. Baran, *Spectrochim. Acta A,*2006,**64,**73.
18 M. Drozd, *Spectrochim. Acta A,*2006,**65,**1069.
19 J. M. Adams and V. Ramdas, *Acta Crystallogr.*1976,**B32,**3224.

20 J. M. Adams and V. Ramdas, *Acta Crystallogr.*1978,**B34,** 2150.
21 J. M. Adams and R. W. H. *Acta Crystallogr.*1974,**B30,**2191.
22 V. Sivashankar, R. Siddheswaran and P. Murugakoothan, *Mater. Chem. Phys.* 2011, **130,** 323.
23 P. Dera, A. Katrusiak and M. Szafran ski, *Pol. J. Chem.*2000,**74,**1637.
24 M. Drozd and J. Baran, *Spectrochim. Acta A,*2006,**64,**867.
25 A. Katrusiak andM. Szafranski, *Acta Crystallogr.*1994,**C50,**1161.
26 M. Drozd, *J. Mol. Struct. Theochem.*2005,**756,**173.
27 J. H. Bryden, *Acta Crystallogr.*1957,**10,**677.
28 A. Akella and D.A. Keszler, *Acta Crystallogr.*1994,**C50,**1974.
29 R. E. Khomaa, V. O. Gelmboldta, V. N. Baumerd, O. V. Shishkind andL. V. Koroevaa, *Russ J. Inorg. Chem.*2013,**58,**843.
30 J. M. Adams, *Acta Crystallogr.*1977,**B33,**1513.
31 M. Koskinen,I. Mutikainen and H. Elo, *Z. Naturforsch.*1994,**49b,**556.
32 I. Mutikainen, M. Koskinen and H. Elo, *Pharmazie,*1994,**49,**739.
33 J. T. Koskinen, M. Koskinen, I. Mutikainen, P. Tilus, B. Mannfors and H. Elo, *Z. Naturforsch.*1997,**52,**1259.
34 T. Todorova, O. Krocher and B. Delley, *J. Mol. Struct. Theochem.*2009,**907,**16.
35 M. Koskinen, I. Mutikainen, P. Tilus, E. Petittari, M. Korvela and H. Elo, *Fur Chemie.*1997,**128,**767.
36 Z. Machackova, I. Nemec, K. Teubner, P. Nemec, P. Vanek and Z. Micka, *J. Mol. Struc.*2007,**832,**101.
37 J. Zyss, J. Pecaut, J. P. Levy and R. Masse, *Acta Crystallogr.*1993,**B49,**334.
38 T. Kolev, Z. Glavcheva, R. Stahl, H. Preut, P. Bleckmann and V. Radomirska, *Acta Crystallogr.*1997,**C53,**IUC9700010.
39 T. Kolev, H. Preut, P. Bleckmann and V. Radomirska, *Acta Crystallogr.*1997,**C53,**805.
40 G. Smith, U. D. Wermuth, D. J. Young and P. C. Healy, *Acta Crystallogr.*2007,**E63,** o556.
41 V. V. Adrabinska, E. Obara and T. Lis, *New J. Chem.*2007,**31,** 287.
42 R. Frohlich, G. Mattern and W. Krumbe, *Z. Kristallogr.- Cryst. Mater.*1985,**172,**315.
43 S. Murugavel, G. Ganesh, A. Pandi, S. Govindarajan and R. Selvakumar, *Acta Crystallogr.*2009,**E65,**o548.
44 S. Murugavel, P. S. Kannan, A. SubbiahPandi, S. Govindarajan and R. Selvakumar, *Acta Crystallogr.*2009,**E65,**o454.
45 J. M. Adams and R. G. Pritchadt, *Acta Crystallogr.*1976,**B32,**2438.
46 J. M. Adams, *Acta Crystallogr.*1978,**B34,**1218.
47 J. M. Adams, R. G. Pritchadt and J. M. Thomas, *J. Chem. Soc., Chem. Commun.*1976, 358.
48 R. Selvakumar, S. J. Geib, A. M. Sankar, T. Premkumar and S. Govindarajan, *J. Phys. Chem. Solids,*2015,**86,**49.
49 P. S. Pereira Silva, M. Ramos Silva, J. A. Paixao and A. Matos Beja, *Acta Crystallogr.*2007,**E63,** o2783.
50 L. Golic, I. Leban, S. Detoni, B. Orel and D. Hadzi, *J. Crystallogr. Spectrosc. Res.*1985,**15,**215.
51 M. Drozd and D. Dudzic, *Spectrochim. Acta Part A,*2012,**89,** 243.
52 J. M. Adams andV. Ramdas, *Inorg. Chim. Acta,*1979,**34,**L225.
53 B. Peng, Q. Peng, W. Zhou and Z. Zhou, *Acta Crystallogr Sect E,* 2010, **E66,** o2679.
54 A. Moghimi, H. Aghabozorg and S. Sheshmani, Farshidramezanipour, *Acta Crystallogr.*2005,**E61,**o442.
55 H. Aghabozorg, F. Manteghi and S. Sheshmani, *J. Iran. Chem. Soc.*2008,**5,**184.
56 S. Packiaraj, A. Pushpaveni, C. Senthil, S. Govindarajan and J. M. Rawson, *J. Therm. Anal. Calorim.* 2015,**119,**15.
57 G.H. Jeffery, J. Bassett, J. Mendham and R.C. Denney, "Vogel's Textbook of Quantitative Chemical Analysis",1986, 5th Ed.
58 APEX-II, Bruker AXS, Wisconsin, USA.
59 SAINT, Bruker AXS, Wisconsin, USA, 2001.
60 SADABS, Bruker AXS, Wisconsin, USA, 2007.
61 O. V. Dolomanov, L. J. Bourhis, R. J. Gildea, J. A. K. Howard and H. Puschmann, Olex2: A complete structure solution, refinement and analysis program, *J. Appl. Cryst*. 2009,**42**, 339.
62 G. M. Sheldrick, Crystal structure refinement with SHELXL, *Acta Cryst.* 2015,**C27**,3.
63 SMART, Bruker AXS, Wisconsin, USA, 2001.
64 A. Shirwaikar and R. Govindraju, *BiolPharmBull.*2003,**26,**1424.
65 K. Nagendra Prasad, B. Yang, S. Yang, Y. Chen, M. Zhao and M. Ashraf, *Food Chem.*2009,**116,**1.
66 N. Ching, L. Pan, X.Y. Huang and J. Li, *Acta Crystallogr.*2000,**C56,**1124.
67 R. H. Wiley, "The Chemistry of Heterocyclic Compounds, Pyrazoles and Reduced and Condensed Pyrazoles", 2009.
68 A. M. Sapse, G. Snyder and A.V. Santoro, *Int. J. Quantum.Chem.*1981,**20,** 755.
69 D. D. Perrin, Dissociation Constants of Organic Bases in Aqueous Solution, Butterworths, London UK, 1965.
70 А. А. Субботин, Г.Ф. Рудаков, В.Ф. Жилин, УДК, Том XXIV,2010,**3,**108.
71 S. Vairam and S. Govindarajan, *Thermochim. Acta*,2004,**414,**263.
72 A. S. Mohamed, Goher, A. Adel, Youssef, A. Franz and Mautner, *Polyhedron*,2006,**25,**1531.
73 Yi-Shan Song, Bing Yan and Zhen-Xia Chen, *J. Mol. Struct.*2005,**750,**101.
74 P. Sengupta, S. Ghosh, C.W. Thomas and Mark, *Polyhedron*,2001,**20,**975.
75 A. Zoya, Savel'eva, V. Galina, Romanenko, A. Liliya, Sheludyakova, V. Stanislav and Larionov, *Polyhedron,*2000,**17,**1737.
76 O. Ugono, N. P. Rath and A. M. Beatty, *Cryst. Growth Des,*2009,**9,**4595.
77 B.R. Bhogala, S. Basavoju and A. Nangia, *Cryst.Eng.Comm.* 2005,7,551.
78 L. Scott, G. Childs, P. Stahly, and A. Park, *Mol. Pharm.*2007,**4**, 323.
79 V. S. Senthil Kumar, T. Premkumar, N. P. Rath and S. Govindarajan, *Indian J. Chem., Sec B,*2007,**46B,**141.
80 N. Peica, I. Kostova and W. Kiefer, *Chem. Phys.*2006,**325,**411.
81 I. Kostova, N. Peica and W. Kiefer, *J. Raman Spectrosc.* 2007,**38,**1.
82 K. Saravanan and S. Govindarajan, *J. Therm. Anal. Calorim.*2003,**73,**951.
83 Dong Wang. Li, Feng Tao, Mei-Ling Chang, Qi Liu, Wei Han,Yu-Juan Wu, Dan-Dan Yang and Li-Juan Wang, *J. Coord. Chem.*2012,**65,**923.
84 K. Rajavelu and P. Rajakumar, *J. Mater. Chem.*2015,**3,**3340.
85 M.R. Fazeli, G. Amin, M.M.A. Attar, H. Ashtiani, H. Jamalifar and N. Samadi, *Food Control.*2007,**18,**646.
86 J. Gabrielson, M. Hart, A. Jarelov, L. Kuhn, D. McKenzie and R. Mollby, *J. Microbiol. Methods*,2002,**50,** 63.
87 T. Premkumar and S. Govindarajan, *World J Microbiol Biotechnol.*2005,**21,**479.
88 T. Premkumar and S. Govindarajan, *World J Microbiol Biotechnol.*2006,**22,**1105.
89 V. Bondet, W. Brand-Williams and C. Berset, *Lebensm, Wiss. u.-Technol.*1997,**30,**609.
90 Z. Zhong, Z. Zhong, R. Xing, P. Li and G. Mo, *Int. J. Bio. Macomol.*2010,**47,**93.

91 W. Shen, Q. Qiu, Y. Wang, M. Miao, B. Li, T. Zhang, A. Cao and Z. An, *Macromol, Rapid. Comm.*2010,**31,**1444.